A chemometric approach using I-optimal design for optimising Pb(II) removal using bentonite-chitosan composites and beads

MAJIYA, Hassan, CLEGG, Francis <http://orcid.org/0000-0002-9566-5739> and SAMMON, Chris <http://orcid.org/0000-0003-1714-1726>

Abstract

This paper reports adsorption studies of Pb (II) ions onto Bentonite-Chitosan (Bt-Ch) composites or beads when using an I-optimal design experiment approach. Three adsorption factors (pH, adsorbent dosage, and initial concentration) were optimised whilst simultaneously investigating multiple adsorbents. The Bt-Ch composites and beads (type A and B) adsorbents were made using weight ratios 90%/10% and differed characteristically due to their preparation methods of solution blending and precipitation, respectively. A batch procedure was used for adsorption experiments, and the amounts of Pb (II) ions (adsorbed onto Bt-Ch composites/beads) were analysed using inductively coupled plasma optical emission spectrometry (ICP-OES). Adsorption experimental parameters were analysed and optimised by using a response surface method (I-optimal design) generated from Design-Expert® 13.0 software. The main achievements of this study were to intensify the understanding and application of I-optimal experimental designs, which allow simultaneous determination of adsorption capacities and efficiencies across multiple adsorbents in an economical manner. A reduced quadratic model provided the best fit for the experimental data and exhibited minimal deviation between predicted and experimental values. This was evidenced by the very small covariance (CV) values of 1.81% and 1.33% observed for adsorption capacity and adsorption efficiency, respectively, also suggesting high reproducibility. It was observed that the adsorption factors studied (pH, adsorbent dose, and initial concentration) have a more pronounced effect on the adsorption capacity (F-value = 714.37) compared to adsorption efficiency (F-value = 140.62). Adsorbent dosage was found to have the greatest effect on adsorption capacity, while the initial pH of Pb (II) solution had the greatest effect on adsorption efficiency. Under optimal conditions, the adsorption capacities of beads-A (73.2 mg/g) and beads-B (77.6 mg/g) were found to be higher than that of the corresponding composite (51.7 mg/g). Whilst the optimum adsorption efficiency values for all three adsorbents were ~100% (with ranges of pH 2-5, initial concentrations 50-200 mg/L and adsorbent dosage 0.05-0.5 mg). The desirability indexes for the optimised conditions for these respective responses (and each adsorbent) were found to be within the ranges of 0.892 – 0.974 and 0.945 – 0.967 for adsorption capacity and adsorption efficiency, respectively. These high desirability index values for both responses indicate that the optimised conditions lead to very good performance for both measures**.** The information

obtained in this study provides detailed understanding of the adsorption phenomena of the adsorbents studied. It gives confidence in the use of I-optimal designs to be applied as a chemometric tool for the specific adsorbents studied herein and others.

Keywords: I-optimal design, Pb (II) adsorption, Bentonite-Chitosan composites

1.0 Introduction

The contamination of water by toxic metals, like lead (Pb), exceeding permissible limits is an issue of great concern to the public and health implications. The major source of Pb contamination in water (and other environmental media) can be traced to the effluents emanating from battery recycling plants, metal mining, and electronic assembly plants; its cumulative effect can result in brain damage, dysfunction of the kidneys, liver and central nervous system in humans (El Kaim Billah et al., 2024; El KaimBillah et al., 2021; Fu and Wang, 2011; Hassan et al., 2015; Liu et al., 2016; Majdoubi et al., 2023; Ngah and Fatinathan, 2009; Nuhu et al., 2014; Sallau et al., 2014; Sharma and Lee, 2013). Adsorption with the combined use of functional composites (made from chitosan biopolymers and bentonite clays) seems to be a promising technique for removal of toxic metals (e.g., Pb) from water (Hao et al., 2018; Jacob et al., 2018; Lata and Samadder, 2016; Liu et al., 2016; Nonkumwong et al., 2016; Wang et al., 2016; Yang et al., 2020). The combination of the biopolymer chitosan with other materials (such as clay) has been reported to improve its chemical and mechanical stability, which in turn also enhances its adsorption capacity. The presence of amine ($-NH_2$) and hydroxyl (-OH) functional groups in the chitosan structure contributes to both polyelectrolyte and chelating properties (Bambaeero and Bazargan-Lari, 2021; Majiya et al., 2019; Majiya, 2017; Pillai et al., 2009; Pooladi and Bazargan-Lari, 2020). Modifications with chitosan performed to date to improve their sorption properties include the incorporation of other sorptive materials, such as clays (Liu et al., 2015; Lourdes Dalida et al., 2011; Rusmin et al., 2015), hydroxyapatite (Bambaeero and Bazargan-Lari, 2021; Pooladi and Bazargan-Lari, 2023, 2020), tripolyphosphate (Ngah and Fatinathan, 2009), polyvinyl chloride (Popuri et al., 2008), and fluorapatite (El KaimBillah et al., 2021)

Adsorption can be extremely complicated and is characterised by various parameters (or termed factors), which have significant influence on adsorbents effectiveness and efficiency (Aydin and Aksoy, 2009). These parameters are critical to a successful adsorbent and therefore finding the optimum values of the operating parameters (conditions) to get the optimum pollutant removal efficiency becomes crucial (Anupam et al., 2011). Thus, process optimisation becomes a vital activity to determine the values of the design parameters (e.g. pH, pollutant concentrations, adsorption time) at which the responses (e.g. maximum adsorption) reach their optimum levels (Anupam et al., 2011; Aydin and Aksoy, 2009).

The traditional and current strategy of conducting experimental work is typically recognised by analysing the change in one factor at a time, in this approach one factor is varied while the other factors are maintained constant (Maleki and Karimi-Jashni, 2020). When studying multiple factors, this approach involves a large number of experiments and leads to an unnecessary waste of resources (e.g. time and chemical reagents). In addition, the effect of one factor might be dependent on the level of other factors, i.e., a factor interaction effect. The use of a one variable at a time approach may therefore often miss important conclusions about the effect of one experimental factor when the level of another factor is changed. In essence, the process optimisation becomes inefficient and there is difficulty in finding the true optimum with a reasonable number of experiments and time (Maleki and Karimi-Jashni, 2020; Montgomery, 2013; Morgan, 1991).

To overcome the limitations discussed above, statistical design of experiments (DoE) can be utilised. Response Surface Methodology (RSM) is one technique used to investigate optimal conditions and combined interaction effects of significant factors for adsorption (and other similar processes). In RSM the values (levels) of each factor are varied in each experiment following a systematic experimental plan. Then an empirical model is fitted to the multivariate experimental data, which is used to obtain a better understanding of the system studied. This has the advantage of evaluating relatively large numbers of factors in a smaller number of experiments and essentially offers better detection and more precise evaluation of factor interactions and process optimisation (Ben-Khalifa et al., 2019; Glyk et al., 2015; Goupy Jacques, 1993; Landdaburu-Aguirre, 2012; Montgomery, 2013; Morgan, 1991; Morgan et al., 1989). A good experimental design is essential for any optimisation process. Classical RSM

designs, such as Central Composite design (CCD) and Box-Behnken design (BBD), can be challenging to map onto experimental scenarios and require a large number of experimental runs for multiple adsorbent samples. Some DoE studies have been published regarding optimising the absorption process to remove heavy metal ions (or other pollutants) from aqueous solutions, and the response surface methods employed to date include CCD (Ahmad and Hasan, 2016; Anfar et al., 2017; Ayushi et al., 2017; Gusain et al., 2014; Yus Azila et al., 2008; Zbair et al., 2019) and BBD (Ahmadi et al., 2014; Rahimi et al., 2015).

To address these challenges, an optimal design (a type of RSM) was used instead. Optimal designs are more flexible and require fewer experimental runs, making them less time-consuming to perform, especially when testing multiple, different adsorbent samples (Goos Peter, 2011; Jensen, 2018; Montgomery, 2013). Two of the commonly used criteria (in optimal design) are the D-criterion and I-criterion. Both of these criteria have distinct characteristics; the D-criterion deals with the variation of factor impacts, while the I-criterion is concerned with the accuracy of predictions (Goos Peter, 2011; Mancenido et al., 2019; Smucker et al., 2018). This implies that I-optimal designs are advantageous for response surface methods when concerned with more accurate predictions as they result in reduced average variance for predictions over the experimental range (as used herein).

While previous studies have employed classical designs of response surface methodology (RSM) for adsorption optimisation, they have always focused on using only one adsorbent at a time. This study introduces and investigates I-optimal design for the optimisation of adsorption parameters with multiple adsorbents simultaneously. This involved the impact of the adsorption factors including pH, adsorbent dosage, and initial concentration on the removal of Pb (II) ions by various novel adsorbents (Bt-Ch composites or beads). The I-optimal experimental designs were generated from Design-Expert® 13.0 software to study the effects of the aforementioned adsorption factors and optimise the removal of Pb (II) ions from aqueous solutions. The optimum conditions were estimated by a numerical optimisation tool and were adjusted by changing the significance of each response involved. The use of I-optimal design could offer several advantages, including fewer experimental runs, improved prediction accuracy, and serve as a model for future adsorption studies.

2.0 Materials and Methods

Lead (II) nitrate (≥ 99.95%), sodium hydroxide (reagent grade, 97%, pellets), and the stock standard solution of Pb (II) for inductively coupled plasma-optical emission spectrometry (ICP-OES), were all obtained from Merck, UK, while nitric acid (HNO_3 69% w/v; specific gravity = 1.41) was obtained from Fisher Scientific, UK. Both nitric acid and sodium hydroxide were used to prepare aqueous acidic and basic solutions, respectively. All preparations were made using deionised water.

2.1 Adsorbent

The three different adsorbent samples tested for Pb (II) removal were Bt-Ch composites, beads-A and beads-B, and labelled as X, Y and Z, respectively. As described in a previous study (Majiya, 2022; Majiya et al., 2023), Bt-Ch composites and beads were prepared by combining bentonite clay and chitosan biopolymer through solution blending and precipitation methods, respectively. These materials were produced by changing the starting compositions in the weight ratios of 90/10, 70/30, and 50/50. The beads were further subdivided into beads-A and beads-B, which were formed by adding bentonite suspension or bentonite powder, respectively, to the solubilised chitosan solution. The detail descriptions of the preparation procedures are shown in the Supplementary section (Table S1). The characterisation of these adsorbents has previously been reported in detail (Majiya, 2022; Majiya et al., 2023). In this study, the three adsorbent samples selected for adsorption tests were of weight ratio 90/10 because after preparation they all contained similar amounts of chitosan. This therefore allowed the design experiments to focus on assessing the effects of different preparation procedures of the adsorbents. For example, results showed that chitosan was intercalated within the interlayer space of the bentonite for Bt-Ch composites and Bt-Ch beads-A, but less intercalation of chitosan was observed for Bt-Ch beads-B.

2.2 Adsorbate solution preparation

The stock solution (1000 mg/L) of Pb(II) ions was prepared by dissolving 1.599 g of lead (II) nitrate in ultrapure deionised water and preserved with 10 ml of aqueous 5% w/v HNO_3 solution as described in a previous study (Majiya et al., 2023). This concentration was chosen because it allowed accurate weighing and minimal dilution requirements to obtain the concentrations for calibration standards and working solutions. Aqueous working solutions were prepared daily from the stock solution by serial dilution.

2.3 Batch adsorption experiments

In this study, batch adsorption experiments were used to assess the adsorption capacity and efficiency of Bt-Ch composites/beads towards Pb (II) ions. The adsorption experiments were designed based on I-optimal designs, as shown in the Supplementary section (Table S2).

The pH of the Pb (II) solution requires careful consideration in this study. At pH > 7 the predominant species of Pb (II) ions are $Pb(OH)^{+}$, $Pb(OH)_2$, and $Pb(OH)_3^{-}$, these have tendency to precipitate and so could therefore lead to erroneous conclusions (Yang et al., 2010). Even at pH 6, a partial precipitation of Pb (II) solution was observed at the highest Pb (II) concentration (250 mg/L) investigated. To ensure that Pb (II) ions were removed only by adsorption processes without the effect of precipitation, the adsorption experiments were carried out within the range of pH 2-5. Adsorption experiments were conducted in cleaned and sterilised Nalgene centrifuge plastic tubes (50 mL capacity). The centrifuge plastic bottles together with their contents were agitated for specified times using a Gyrotory Water Bath shaker (Model G76D; New Brunswick Scientific, Edison. N.J. U.S.A). After that, the mixtures were centrifuged (using a Sorvall RC6 Superspeed Centrifuge) at 3000 rpm for 5 minutes and the supernatant collected and stored in cleaned and sterilised Fisherbrand PP centrifuge tubes (15 mL capacity) appropriately labelled for analysis of Pb (II) ions. The quantitative measurement of Pb (II) ions was carried out by ICP-OES (Agilent 5110 ICP-OES) using wavelength 220.353 nm, axial viewing mode and linear weighted calibration fit as measurement conditions. Standard solutions of 10, 20, 50, 100, 200, and 300 mg/L Pb (II) were used for the calibration curve of the Pb (II) measurements.

The amounts of Pb (II) ions per unit mass of adsorbent and percentages of adsorption performance (%) were calculated using Equations 1 and 2, respectively.

$$q_e = \frac{C_i - C_f}{M} \times V \quad (1)$$

$$\%\ \text{Adsorption} = \frac{C_i - C_f}{C_i} \times 100 \quad (2)$$

Where q_e (mg Pb(II) ions g^{-1} adsorbent) is the adsorption capacity, and C_i and C_f (mg L^{-1}) are initial and final concentrations of the Pb(II) ions before and after the adsorption experiment, respectively. V (L) is the volume of solutions and M (g) is the mass of the adsorbent.

2.4 Response Surface Methodology

2.4.1 Optimisation stage

An adsorption study using screening designs (two-level fractional factorial) was performed to examine six potential factors namely, pH, initial concentration, agitation rate, temperature, adsorbent dosage, and agitation time for their significance. The detailed description of the screening experiment is discussed elsewhere (Majiya, 2022) yet the results are presented in the Supplementary section (Figure S1). The screening experiment identified only three variables (pH, initial concentration, and adsorbent dosage) to have a significant effect. Therefore, one categoric factor (adsorbent type) and three numeric factors (pH, initial concentration, and adsorbent dosage) were incorporated into the response surface experiment (Table 1).

2.4.2 I-optimal Experimental Design

Using Design-Expert® 13.0 software, an I-optimal experimental design was constructed, consisting of 28 experimental runs with five replicates. This design is detailed in the Supplementary section (Table S2). Each factor level combination was in a randomised order. A sequential model fitting process was then performed using three different tests (sequential model sum of squares, lack of fit tests, and model summary statistics) to evaluate the competency of the models. The results from this showed the best fit to be a second-order polynomial model, which has main effects, two-factor interactions, and quadratic terms. The quadratic terms capture the curvature in the relationship between the response (adsorption capacity or efficiency) and the experimental variables. In summary, the equation model was defined as:

$$Y = \alpha + aA + bB + cC + dD + abAB + acAC + adAD + bcBC + bdBD + cdCD + aaA^2 + bbB^2 + ccC^2 \quad (3)$$

where Y (e.g., Pb-adsorption capacity, mg/g or efficiency, %) is the measured response associated with every variable level combination, **α** is the intercept (mean value), A, B, C and D are the main factors (A = pH of Pb (II) ion solution; B = adsorbent dosage; C = initial concentration of Pb (II) ion solution; D = adsorbent type). AB, AC, AD, BC, BD, CD are the two-factor (binary) interactions; A^2, B^2, C^2 are the quadratic numerical (quantitative) factors; and

a, b, c, d or ab, ac, ad, bc, bd, cd or aa, bb and cc are the coefficients of the main factors, interaction factors, and quadratic numerical factors, respectively.

Analysis of variance (ANOVA) was also carried out to assess and check the significance (by p- and F-values) and adequacy (lack-of-fit test and correlation coefficients) of the quadratic model. Through this process the non-significant terms in the quadratic model can be removed and thus improve predictions. Perturbation plots were used to visualise the effect of each significant quantitative factor on Pb adsorption by Bt-Ch composites and beads. 3D surface plots and 2D contour plots were used to visualise the interactive influence of the significant factors on adsorption by Bt-Ch composites and beads.

2.5 Optimisation and desirability function of adsorption parameters

Generally, optimum adsorption conditions are determined by a numerical optimisation method and one of the popular strategies is to use the simultaneous optimisation technique, which was put forward by Derringer and Suich (1980) (Montgomery, 2013; Myers et al., 2016). This method adopts an objective function D, often referred to as the desirability function, which transforms calculated response into a free scale value (d_i) called desirability (Myers et al., 2016). The desirability ranges from zero to one (i.e., least to most desirable, respectively). The factor settings with best total desirability are the optimal conditions. The simultaneous objective function is a geometric mean of all transformed responses, which is given as;

$$D = (d_1 \times d_2 \times d_3 \ldots\ldots d_n)^{\frac{1}{n}} \qquad (4)$$

where D is the desirability function, d_1, d_2, d_3 and d_n are the desirability ranges for each response, and n is the number of responses in the measurement.

3.0 Results

3.1 Surface response approach: I-optimal design

I-optimal experimental design was used to optimise conditions for the adsorption of Pb (II) ions on Bt-Ch composite and bead samples. The experimental design investigated the respective (and combined) effects of pH, initial concentration, and adsorbent dosage on the

adsorption of Pb (II) ions by Bt-Ch composites/beads. The adsorption capacity (mg/g) and efficiency (%) were evaluated as a function of these three independent factors. The results of the 28 experimental runs, along with their corresponding experimental and predicted responses (adsorption capacity and adsorption efficiency) are presented in the Supplementary section (Table S2).

Sequential model fitting was used to assess the credibility and reliability of various models, including linear, 2-factor interaction, quadratic, and cubic. Three different fittings were employed: sequential model sum of squares, lack of fit tests, and model summary statistics. The results of these fittings for both responses (adsorption capacity and adsorption efficiency) are presented in Tables S3 and S4, respectively. The sequential model sum of squares approach generally suggests the best model as being that with the highest F-value and lowest p-value. For the lack of fit tests, the suggested model should have the lowest F-value and highest p-value to ensure statistical insignificance. Whilst with model summary statistics, the suggested model is based on the lowest standard deviation and highest correlation coefficients (R^2, $R^2_{adjusted}$, and $R^2_{predicted}$). Based on these criteria, the quadratic model was found to provide the best fit for both responses.

3.2 Analysis of variance (ANOVA)

After the model was chosen, analysis of variance (ANOVA) was used to evaluate the model's overall performance and the significance of individual terms (main, interactive, and quadratic effects). Summaries of the ANOVA results for the adsorption capacity and adsorption efficiency of Pb (II) ions by Bt-Ch composites/beads with respect to the full and reduced quadratic models are presented in the Supplementary section (Tables S5 – S8). The ANOVA tables show the F-values, p-values, and degrees of freedom (df) for the overall model (top row), each factor (next four rows), and the interactions (following eight rows). The F-value is a measure of the amount of variation between the factors and the response. The p-value is a probability value that indicates the significance of the difference between the effects of the factors on the response. A p-value of less than 0.05 indicates that the difference is statistically significant (Ahmad and Hasan, 2016; Montgomery, 2013). The ANOVA table also includes several other statistics that can be used to interpret the results of the analysis. These statistics include the mean square error, adjusted R-squared, and predicted R-squared.

3.2.1 Full quadratic models

The full quadratic model is assessed when non-significant terms (as indicated by the ANOVA) have not yet been removed from the model. The ANOVA tables for the full quadratic model of adsorption capacity and adsorption efficiency are presented in Tables S5 and S7 of the Supplementary section. The full-quadratic models were deemed significant for both adsorption capacity and adsorption efficiency with F-values of 658.45 and 120.97, respectively. Pb-adsorption capacity (Table S5) was affected linearly by pH (A), adsorbent dosage (B), initial concentration (C), and adsorbent type (D). Binary interactions were observed between; pH-adsorbent dosage (AB), pH-adsorbent type (AD), adsorbent dosage-initial concentration (BC), and adsorbent dosage-adsorbent type (BD). Significant quadratic effects were also noted with the pH (A^2), adsorbent dosage (B^2), and initial concentration (C^2). For adsorption efficiency (Table S7) linear effects were also observed with pH (A), adsorbent dosage (B), and initial concentration (C), but not adsorbent type (D). Binary interaction effects were the same as for adsorption capacity, but with the addition of CD, only two quadratic effects (A^2 and B^2) were found to be significant (not C^2).

3.2.2 Reduced quadratic models

The model reduction was performed where appropriate by deleting or reducing non-significant terms to improve the proposed model (Design-Expert® 13.0 software). The ANOVA tables for the reduced quadratic model of adsorption capacity and adsorption efficiency are presented in Tables S6 and S8 of the Supplementary section. As shown the importance of the terms in the quadratic models varied, and their significance was assessed through F-value and p-values. If the p-values were greater than 0.10 then the model terms were deemed not significant and so were removed from the model. For adsorption capacity, the binary interactive term AC (P-value = 0.40 > 0.10; Table S5) was ruled out, and the model F-value improved to 714.37 from 658.45 (Tables S6 and S5, respectively). For adsorption efficiency, AC (P-value = 0.92 > 0.10; Table S7) and C^2 (P-value = 0.23 > 0.10; Table S7) were removed, and the model F-value increased to 140.62 from 120.97 (Tables S8 and S7, respectively). Although the p-value for factor-D (adsorbent type) was slightly greater than 0.10 (P-value of factor-D = 0.19; Table S7 and S8) it was not deleted from the model because it is an important

categorical factor, which supports the hierarchy of other significant terms such as AD, BD, and CD.

The adequacies of these reduced models were also checked with lack-of-fit tests (Table S6 and S8, for adsorption capacity and adsorption efficiency, respectively). The non-significant lack-of-fit values for adsorption capacity (F = 0.4012; P = 0.8515) and adsorption efficiency (F = 0.771; P = 0.6368) suggest that both models are adequate to explain data within the experimental design, since the p-values were greater than 0.05 (Yus Azila et al., 2008).

Another assessment of the adequacy of these modified quadratic models are the correlation coefficients R^2, $R^2_{adjusted}$ and $R^2_{predicted}$, these are presented in Tables S6 and S8, for adsorption capacity and adsorption efficiency, respectively. When a repressor variable is eliminated (i.e. a variable that increases the predictive validity of another variable) in statistical modelling, the coefficient of determination decreases, and a high R^2 value does not necessarily confirm a good regression model. Therefore, R^2_{adj} is preferred in evaluating the regression model fit as it does not necessarily increase with additional variables (Rahimi et al., 2015). The current study revealed a high dependence and correlation between the observed and predicted values of the responses (i.e., adsorption capacity or adsorption efficiency) with a high R^2 value of 0.99. The R^2_{adj} values (0.99 for both adsorption capacity and adsorption efficiency) indicated that the independent variables explained approximately 99% of the total variation in Pb removal (uptake and efficiency), while only 1% of the variation could not be accounted for by the model. Also, the predicted R^2 (0.99 and 0.95; for adsorption capacity and adsorption efficiency, respectively) were in reasonable agreement with adjusted R^2 (0.99 for both adsorption capacity and adsorption efficiency).

The coefficient of variance (CV) is expressed as a percentage and represents the ratio of the standard error of estimate to the mean value of the observed response. When it does not exceed 10%, it is considered to be reproducible (Yus Azila et al., 2008). In this study, the small values of CV (1.81% and 1.33%; for adsorption capacity and adsorption efficiency, respectively) implies that deviation between the predicted and experimental data values were minimal and highly reproducible. Adequate precision measures the signal-to-noise ratio, and a ratio greater than 4 is desirable (Design-Expert® 13.0 software). For these models, the

ratio value was found to be 104.77 and 43.03 for adsorption capacity and adsorption efficiency, respectively, which indicates an adequate signal for Pb adsorption.

The mathematical relationships between these three studied independent factors (i.e., pH, initial concentration, and adsorbent dose) and the responses (i.e., adsorption capacity and adsorption efficiency) were also provided by the Design-Expert® 13.0 software. The quadratic equations in terms of actual factors (with regards to respective adsorbents) which describes the various parameters regarding the Pb (II) adsorption onto Bt-Ch composites are all shown in Equations 5 (adsorption capacity) and 6 (adsorption efficiency). The equations for other adsorbents (beads A and beads B) are presented in the Supplementary section (see Equations S1- S4). The actual values are the experimental or measured values of the adsorption capacity and adsorption efficiency obtained for Bt-Ch composites/beads, and were determined experimentally using Equations 1 and 2, respectively, while, predicted values were generated by using Equations 5 (adsorption capacity) and 6 (adsorption efficiency).

$$Log_{10}(\text{Adsorption capacity})X = 0.0776 + 0.4689\text{A} - 2.7332\text{B} + 0.00648\text{C} - 0.1562\text{AB} + 0.0037\text{BC} - 0.05204\text{A}^2 + 2.5178\text{B}^2 - 0.0002\text{C}^2 \quad (5)$$

$$Log_{10}(\text{Adsorption efficiency})X = 0.6258 + 0.5250\text{A} + 2.3522\text{B} - 0.0012\text{C} - 0.2015\text{AB} + 0.0034\text{BC} - 0.0557\text{A}^2 - 2.4599\text{B}^2 \quad (6)$$

Although the equations generated by the response surface designs may not accurately predict the actual value when computing factor values due to noise, model limitations, or complexity, they still reveal essential information about the influence of each factor (Goos Peter, 2011). In the above equations, the coefficient values represent strength, and positive or negative signs signify the nature and influence of respective terms on the response. A positive effect for a factor means that the response is improved by increasing the factor level. A negative effect indicates that an increase in the factor level has an inhibitory effect on the response (Bajpai et al., 2012; Maleki and Karimi-Jashni, 2020; Sarkar and Majumdar, 2011). As can be seen from Equation 5, the Pb adsorption capacity (mg/g) increases with pH (A) and initial concentration (C) but decreases with adsorbent dosage (B) (this is also noted in the coefficient estimate of A, B, and C in Table S6). For Pb adsorption efficiency (%) pH (A) and adsorbent

dosage (B) increases but initial concentration (C) decreases when increasing the factor level (also see the coefficient estimates of A, B, and C in Table S8).

3.3 Diagnostic analysis of fitted reduced quadratic model

To check the adequacy of the selected model for the appropriate approximation of the real data, diagnostic plots provided by the Design-Expert 13.0 software, such as a normal probability plot of residuals can be used (Maleki and Karimi-Jashni, 2020). Figure S2 (a) and (b) in the Supplementary section depict the normal probability plot of the residuals (predicted value from model minus actual value) for both adsorption capacity and adsorption efficiency, respectively. These plots are used to check the normality of the data. As seen from these plots, the data points lie near a diagonal straight line without little deviation. Furthermore, residuals are used in model analysis to compute error by examining the disparity between predicted values and experimental data. Independent plots can be used to verify residual plots against the analyses (runs) of the experiments. The evaluation of model adequacy heavily relies on residuals obtained from the experimental design. Figure S3 (a) and (b) in the Supplementary section depict the comparative analysis of the predicted and experimental values for both adsorption capacity and adsorption efficiency based on the developed model. The percentage errors between the actual and predicted values ranged from -2.99% to +3.18% for adsorption capacity and -5.00% to +3.12% for adsorption efficiency.

3.4 Perturbation plot and the effects of the main factors on Pb adsorption

Perturbation plots can be utilised to visualise the effect of quantitative factors (pH, adsorbent does and initial concentration) on analysed responses (adsorption capacity and adsorption efficiency), they are simplistic, but useful for assessing the impact of the various factors at a specific location in the design space. In effect, the response is displayed by changing a single factor while all other variables remain constant. When the line of a factor in a perturbation plot has a steep slope or curvature, it indicates that the response is easily influenced by that factor. Conversely, a relatively flat line indicates that the factor has little impact on the response. If there are multiple factors, the perturbation plot can therefore be used to identify which factors have the greatest effect on the response.

The perturbation plots showing the effect of each quantitative factor on the adsorption capacity (mg/g) and adsorption efficiency (%) of Pb (II) ions by Bt-Ch beads-A (adsorbent Y) are shown in Figure 1 (a) and (b), respectively. The perturbation plots (concerning the same responses) obtained for the other two adsorbent samples (i.e., composites and beads-B designated as adsorbents X and Z, respectively) are shown in the Supplementary section (see Figure S4). It is observed in the perturbation plots that the adsorption efficiency (%) exceeds 100%, which is not theoretical possible and so these may be due experimental errors or variations in the measurement, however it does represent near to 100% adsorption efficiency.

Generally, the line plots for each factor (A, B or C) are similar for each adsorbent for either adsorption capacity or adsorption efficiency. The most significant factor for adsorption capacity is adsorbent dosage (B) as indicated by the sharp decreasing slope from a negative to positive deviation from the reference point. The perturbation plots for pH (A) and initial Pb concentration (C) exhibited almost flat curves, indicating that changes in these factors had less impact on adsorption capacity, but still remain crucial in affecting the adsorption process. The non-linear line plots within the adsorption capacity data for pH, adsorbent dose, and initial concentration were due to the influence of the quadratic terms in their modelled equations (A^2, B^2 and C^2, respectively) as indicated as significant in the ANOVA Table (Table S6).

For adsorption efficiency, line plots for both pH (A) and adsorbent dosage (B) show steep slopes compared to initial concentration indicating these are the most significant factors affecting the response of the adsorption efficiency. The line plot for initial concentration is linear and reflects its non-significance as a quadratic term in the modelled equation (Table S8).

3.5 The 3D response surface and 2D Contour plots analysis

To help visualise the interactive influence of the significant variables on the adsorption of Pb (II) ions onto Bt-Ch composites/beads, 3D response surface and 2D contour plots can be used. These plots are graphical representations of the regression equation and show the simultaneous interaction effect of two variables (on responses), while maintaining the other variable constant (Ahmad and Hasan, 2016; Verma et al., 2017). Examples of the 3D response

surface and corresponding contour plots for adsorption capacity are presented in Figures 2 and 3, respectively, and Figures 4 and 5 illustrate the same for adsorption efficiency. In the context of 3D response surface plots, it is not possible to vary all three factors simultaneously; one factor must be fixed. For instance, when visualising the 3D response surface plot for the interaction effect of pH and adsorbent dosage, a constant initial concentration of 200 mg/L was fixed for adsorption capacity (Figure 2a) and 150 mg/L for adsorption efficiency (Figure 4a). Similarly, for the 3D response surface plot depicting the interaction effect of adsorbent dosage and initial concentration, a constant pH of 4.5 was fixed for both adsorption capacity and adsorption efficiency (Figure 2b and 4b, respectively). This allows a clearer view of how the other two factors interact. As mentioned above, the adsorption efficiency (%) should be no more than, very close to, or identical to 100%, but the 3D surface plots (for adsorption efficiency, %) did show data marginally above 100%. This could be down to inaccuracies found in the set-up of the experimental model applied or to any variance related to experimentation.

3.5.1 Interactive effect of pH and adsorbent dosage

As already discussed in Section 3.2.2 solution pH (A) and adsorbent dosage (B) have an interactive effect (interaction AB, $p < 0.0001$) on both the adsorption capacity (mg/g) and adsorption efficiency (%) of Pb ions (Tables S6 and S8). It is not unexpected for pH to have an effect since it has been widely reported that the initial pH of the adsorbate solution plays a significant role in the adsorption process of heavy metal ions from aqueous solution (Chen et al., 2018). In this study, the effect of pH was examined within the range from pH 2 to 5, and at the lower adsorbent dosages (with constant 200 mg/L initial concentration), both the respective adsorption capacity and removal efficiency were found to increase with increasing pH for Bt-Ch beads-B (adsorbent Z), as shown in the 3D response plots, Figures 2a and 4a, and 2D contour plots Figures 3a and 5a. Thus, the lowest loading capacity (mg/g) and removal efficiency (%) of Pb ions was obtained at a lower pH (2) for low adsorbent doses, this is likely due to competition from hydronium ions (H_3O^+) and protonation of adsorbent active sites such as the silanol groups present on bentonite and the amino groups (pKa = 6.0 to 6.5) present on the chitosan biopolymer (Abollino et al., 2003; Wang et al., 2008). As the pH increases, these active sites are largely deprotonated and thereby, encourage more Pb (II)

ions uptake by the adsorbent (Wang et al., 2008). There is also the movement towards lower solubility as pH increases.

At the higher adsorbent doses (0.3 to 0.5 g) the adsorption capacity does not show any significant increase with pH apart from a slight non-linear relationship (Figures 2a and 3a), whereas the adsorption efficiency of Pb ions only slightly increases and then decreases as pH of the solution increases from 2 to 5 (Figures 4a and 5a). As indicated above, the impact of pH on Pb adsorption can vary depending on the size of the adsorbent dosage. While buffering from the adsorbent could play a role, a previous study indicated that, even before adsorption begins, the addition of adsorbents (composites and beads) raises the solution pH (Majiya et al., 2023), which logically should lead to greater Pb adsorption herein. However, this isn't the case. Instead, steric hindrance caused by the close packing and formation of diffusional barriers within the adsorbent is a plausible alternative or contributing factor at play, which could account for the lesser effect of pH on both Pb adsorption capacity and efficiency at higher adsorbent dosages. The non-linear response reflects the quadratic effect of pH (A^2, as noted in Tables S6 and S8 in the Supplementary section). This quadratic effect of pH (A^2) is minimal in comparison to the linear effect of pH (A). The other adsorbents, composites and beads-A, exhibited similar trends within their 3D surface and 2D contour plots for adsorption capacity (Figures S5 and S6) and efficiency (Figures S7 and S8), but differences in adsorption extents were noted. For example, at a pH range of 4 – 5, Bt-Ch composite (adsorbent X) had a Pb uptake of 40 mg/g, while both of the bead's samples (adsorbents Y and Z) had Pb uptakes of about 60 mg/g.

When considering change in adsorbent dosage at lower pH for all adsorbents, the adsorption capacity shows only a slight decrease with increase in adsorbent dose from 0.05 to 0.5 g, but a much larger change and increase for adsorption efficiency (%). The near steady change in adsorption capacity is because the amounts adsorbed are lower than the maximum adsorption capacities and the capacity to adsorb is not greatly affected. The observed higher removal efficiency with increase in adsorbent dosage, is due to the fact that at high adsorbent dose, more adsorbent surface and exchangeable sites for adsorption are available for the Pb (II) ions adsorption (Radnia et al., 2012). At higher pHs, the adsorption capacity decreases more as adsorbent dose increases while the adsorption efficiency generally increases and plateaus as adsorbent dose is increased. The observation that adsorption capacity decreases

more with increasing adsorbent dosage at higher pHs could again be explained in terms of steric hinderance effects, the higher adsorbent levels leading to closer packing and diffusional barriers within the adsorbent. These phenomena could also result in less of a buffering effect (i.e., preventing pH increase). As for the observation that adsorption efficiency first increases and then decreases with increasing adsorbent dosage, this can be attributed to the interplay between multiple factors including saturation of the adsorbent's active sites. At low adsorbent dosages, the adsorbent's active sites are not fully utilised. Again, as the adsorbent dosage continues to increase, the adsorbent particles start to pack together more tightly, leading to the formation of diffusional barriers and steric hindrance, which can counteract the increased availability of active sites.

The influence of adsorbent dosage may have a positive and negative effect on the adsorption capacity and adsorption efficiency, respectively, in a non-linear manner (as reflected in the B^2 coefficient in Tables S6 and S8, respectively in the Supplementary section). In comparison to the linear effect of adsorbent dosage (B), the quadratic effect of adsorbent dosage (B^2) has a lower strength (but opposing sign) for adsorption capacity. However, for adsorption efficiency, the quadratic effect of adsorbent dosage (B^2) has a similar strength (and same sign) in comparison to the linear effect of adsorbent dosage (B).

3.5.2 Interactive effect of adsorbent dosage and initial concentration

The ANOVA analysis (Tables S6 and S8) also showed the adsorbent dosage (B) and initial concentration (C) had an interactive effect (interaction BC, $p < 0.0001$) on both the adsorption capacity and adsorption efficiency of Pb ions. Figures 2b and 4b show the respective 3D response surface plots and Figures 3b and 5b the 2D contour plots for the interaction effect of adsorbent dosage and initial concentration (at constant pH of 4.5) on Pb (II) adsorption capacity and adsorption efficiency for 90%Bt-10%Ch beads-B.

When the initial concentration was low (i.e., 50 mg/L), the adsorption capacity of Pb (II) ions was only influenced a little by the adsorbent dose, but at higher initial concentrations (i.e., 250 mg/L) the adsorption capacity decreased a lot with increasing adsorbent dose. At low initial concentrations, the adsorption efficiency remained high close to 100%, but at higher initial concentrations the adsorption efficiency was lower at lower adsorbent doses. It should be noted that the adsorption efficiency does increase beyond 120%, as discussed above,

which is nonsensical and can be considered at 100%. Similar trends were observed for all the 3D plots of other adsorbents as shown in the Supplementary section (Figures S5 and S7 for adsorption capacity and efficiency, respectively). The larger changes in adsorption capacity at higher initial concentrations can be explained by mass transfer effects, a phenomenon in which the adsorption of most heavy metals (including Pb) becomes an extremely concentration-dependent process (Radnia et al., 2012). The adsorption is driven by a concentration gradient between the medium and the adsorbent material. With less adsorbent, the phenomenon is more likely to happen due to higher competition and thus Pb will migrate more to the adsorbent surface. The decrease in adsorption efficiency can be explained by relatively fewer adsorption sites being available as adsorbent dosage decreases.

At low dosage (0.05 g) and increasing initial concentration (50 to 250 mg/L) the adsorption capacity increases, whilst the adsorption efficiency decreases. Here again, the adsorption capacity is affected by mass transfer effects. At the higher dosages (0.5 g), this has less of an effect and thus why the steady adsorption capacity is observed. At higher adsorbent doses and increasing initial concentration (Figure 4b) maximum adsorption efficiency is reached (percentage is close to 100% or above) as there are more active sites for Pb adsorption (Radnia et al., 2012; Surchi, 2011).,

Although the maximum adsorption capacities here (2D contour plots; Figure 3b) are only based on two factors, it is interesting to note differences in the highest amount of adsorption capacity between the different adsorbents, Bt-Ch beads-B achieved 60 mg/g of Pb uptake within an initial concentration range of 200-250 mg/L (Figure 3b), beads-A achieved the same amount of uptake, but at a lower initial concentration of 200 mg/L, whilst Bt-Ch composites achieved 40 mg/g of Pb uptake with an initial concentration range between 150-200 mg/L (Figure S6d & S6e, respectively). The observed difference in Pb uptake between beads and composites highlights the model's ability to discern adsorption capacity variations arising from chitosan distribution, as reported in a previous study (Majiya et al., 2023). However, these values remain lower than the optimal capacities achievable when considering all three factors, as detailed later. This emphasises the importance of incorporating all significant parameters for optimising experimental conditions.

The influence of initial concentration may have a negative effect on the adsorption capacity in a non-linear manner (C^2, check the coefficient in Table S6 in the supplementary section). In comparison to the linear effect of adsorbent dosage (C), the quadratic effect of adsorbent dosage (C^2) has a lower strength (but opposing sign) for adsorption capacity.

3.6 Optimisation of parameters for Pb (II) adsorption by Bt-Ch composites/beads

To obtain the optimum values of Pb-adsorption capacity and efficiency for the different adsorbents, a numerical optimisation method was used. This method determines the optimal point that maximises the desirable conditions related to the desirability function. The desirability function is a multiple-response approach that calculates an objective function that ranges from 0 to 1 (i.e., from undesirable to target conditions). With this tool, one can combine a favourable set of conditions to achieve optimal experimental conditions that fulfil all goals to the highest extent possible.

The numerical optimisation approach (within the Design Expert® 13.0 software) sets the values of pH, adsorbent dosage, and initial concentration of Pb (II) ions within their ranges, selecting each specific adsorbent (Bt-Ch composites, beads-A and beads-B) and thus maximising (optimising) the adsorption capacity and removal efficiency of Pb (II) ions (Table S9 in Supplementary section). In this study, simultaneous optimisation of the multiple responses was applied, where respective responses (i.e., adsorption capacity or adsorption efficiency) were integrated into the process. Optimum conditions for each response involved were estimated by the numerical optimisation tool that was adjusted by changing the significance (importance) between each response.

Figures S9, S10 and S11 (Supplementary section) show optimised conditions for Bt-CH composites, beads A and beads-B, respectively, when adsorption capacity was considered more important than absorption efficiency (importance = 5 and 1, respectively). The model chose the lowest adsorbent dose within the range, 0.05 g, as the best for Pb uptake by Bt-Ch composites, beads-A, and beads-B, and also selected optimal pH values near to the upper limit of the pH range of 4.5, 4.9, and 4.6, with initial Pb concentrations within the upper range of 216.8, 199.6, and 214.8 mg/L, respectively. At these conditions, the adsorption capacities were 51.67 mg/g, 73.22 mg/g, and 77.56 mg/g, respectively (Figure 6a), with corresponding adsorption efficiencies of 51.41 %, 60.31 %, and 58.99 %, and desirability values of 0.89, 0.96,

and 0.97. Notably, beads-A and beads-B had higher adsorption capacities than their corresponding composites under optimal conditions. As a previous study revealed, both composites and beads prepared in the weight ratio of 90/10 contain the same amount of chitosan (Majiya, 2022; Majiya et al., 2023). While different methods were used to prepare the composites and beads, morphology studies revealed slight varying distributions of chitosan on their surfaces. This explains the differences in optimal adsorption capacities observed among these adsorbents. It could also be stated that the optimal pH values, adsorbent doses, and initial concentrations didn't vary much between the 3 adsorbent types and thus the differences are due to the different adsorbent characteristics.

When the emphasis was placed more on adsorption efficiency (importance = 5) rather than adsorption capacity (importance = 1), as shown in Figures S12, S13 and S14, the optimal conditions chosen by the model for Bt-Ch composites, beads-A, and beads-B were as follows: pH levels of 4.2, 4.9, 4.4; adsorbent doses of 0.25, 0.05, 0.17 g; and initial Pb concentrations of 236.97, 67.97, 140.90 mg/l, respectively. These conditions achieved adsorption efficiencies of 100 % (22.49 mg/g; desirability = 0.95), 100 % (36.30 mg/g; desirability = 0.97), and 100 % (28.33 mg/g; desirability = 0.96), respectively (Figure 6b). Therefore, while the amounts of adsorbent dose and initial concentrations varied considerably, the pH remained consistent across all tested adsorbents in achieving optimal adsorption efficiencies of 99.9%.

It's important to keep in mind that the estimated optimum response values, which include the optimum adsorption capacity and efficiency, may not be optimal in reality due to errors in the estimates and inadequacies of the model. The polynomial equations provided by the model were validated by performing confirmatory adsorption experiments, although only the result of the confirmatory experiment with Bt-Ch composite (adsorbent X) is presented in Table 2. This is because the model only recommended one confirmatory experiment, and it was to be done with adsorbent X. In addition, under selected adsorption conditions, the confirmatory experiments were also independently carried out for the other adsorbents (Y and Z, Bt-Ch beads-A and beads-B, respectively), and their results show that the experimental adsorption values (i.e., adsorption capacity and adsorption efficiency) closely matched the predicted values obtained using this model (see Table S10 in the Supplementary section). This implies that the predicted results were within the accuracy and precision of the design space

(95% for both prediction and confidence intervals), which provides confidence in the reproducibility and accuracy of the analysis.

4.0 Discussion

4.1.Model development and statistical analysis

This study demonstrates that I-optimal design can be a useful tool to simultaneously investigate the impact of various adsorption parameters affecting the removal of Pb (II) ions from aqueous solutions by multiple adsorbents. The three adsorbent samples used for this study were composed from a 90/10 ratio of bentonite to chitosan. Response surface experiments were also conducted for respective samples composed of 70/30 and 50/50 ratios, replicating the exact approach used for the 90/10 samples (Majiya, 2022). For each ratio, all three adsorbent types (composites, beads-A, and beads-B) were tested together in a single experiment. This was performed to ensure that all adsorbents were tested under the same conditions and to avoid any potential bias that could arise from running separate experiments (Majiya, 2022), with this the same number of experimental runs were conducted. It is noteworthy that a single experimental setup could have been utilised with a set of nine adsorbents (combining 90/10, 70/30, and 50/50 ratios for composites, beads-A, and beads-B). With this approach it would have reduced the number of experimental minimising time and chemical usage, though although not tested, it may have compromised the statistical power of the study, making it more challenging to detect significant effects.
The data obtained from model summary statistics suggested that a quadratic model was the most suitable (Tables S3 and S4), and ANOVA confirmed that a reduced quadratic model, obtained by deleting or removing non-significant terms (Design-Expert® 13.0 software) was the most valid to explain the data derived from the two responses concerning the adsorption of Pb (II) ions by Bt-Ch composites or beads (Table S6 and S8). The reduced quadratic models developed in this study were satisfactory for the prediction of Pb (II) ions in the system, with an R^2 value of 0.99 for both adsorption capacity and adsorption efficiency.

Having confirmed the significance of the reduced model for Pb (II) ion removal (ANOVA Table S6 and S8), the main effects of pH, adsorbent dosage, and initial concentration, as well as

their quadratic terms, were also highly significant ($p < 0.0001$). The observed F-value for adsorption capacity (714.37) was significantly higher than that for adsorption efficiency (140.62). This indicates that the studied adsorption factors (pH, adsorbent dose, and initial concentration) have a stronger impact on the amount of Pb adsorbed per unit mass of the adsorbent (adsorption capacity) than on the percentage of Pb removed from the solution (adsorption efficiency). Thus, the adsorption capacity appears to be more sensitive to changes with respect to investigated adsorption factors compared to adsorption efficiency. This sensitivity is reflected in the higher F-values associated with these factors obtained for adsorption capacity, as compared to the F-values observed for adsorption efficiency. One possible reason for the higher F-value observed in adsorption capacity could be the nonlinearity of the model. Specifically, all three investigated factors (pH, adsorbent dose, and initial concentration) have quadratic terms that are significant in the model (A^2, B^2, and C^2, respectively). However, for adsorption efficiency, only two factors (pH and adsorbent dose) have quadratic terms in the model (A^2 and B^2, respectively), which may contribute to the lower F-value.

4.2 Interactions between adsorption parameters, and comparison to previous studies

For adsorption capacity, the adsorbent dosage was the most significant factor affecting the Pb uptake (mg/g) by Bt-Ch composites or beads. Whereas pH was the most significant factor affecting the adsorption efficiency of Pb ions by Bt-Ch composites or beads. There was also strong evidence that two-factor interaction effects involving pH-adsorbent dosage and adsorbent dosage-initial concentration existed, as the p-values for these effects were also less than 0.0001. The implication of this is that the effect of pH is more pronounced at lower adsorbent dosage for both adsorption capacity and adsorption efficiency. At low adsorbent dosages, the adsorbent particles are more likely to be dispersed and thus have more free surface area available for Pb adsorption. This makes them more sensitive to pH changes, as even small changes in pH can alter the electrostatic interactions between these adsorbents and the Pb ions. For adsorbent dosage, the effect with respect to adsorption capacity was more affected at higher pH and higher initial concentration. When the pH level is higher, the adsorbent's ability to buffer is diminished. Consequently, the adsorbent becomes less efficient in maintaining stable pH levels, which in this situation appears to impede the

adsorption of Pb as the amount of adsorbent used increases. At higher initial Pb concentrations, the adsorbent must compete with more Pb ions relative to active sites on the surface, which can limit the adsorption extent, and overall adsorption capacity. However, in terms of adsorption efficiency, the effect of adsorbent dosage was significantly noticed at both lower and higher pH and initial concentrations. Similarly, the effect of initial concentration was observed to be more pronounced at lower adsorbent dosage for adsorption capacity and adsorption efficiency, respectively. Furthermore, the quadratic effects of pH, adsorbent dosage, and initial concentration were observed for adsorption capacity of Pb ions, yet only quadratic effects of pH and adsorbent dosage were observed for adsorption efficiency. These important observations about the behaviours of Pb (II) adsorption by Bt-Ch composites or beads cannot be easily obtained by one-factor-at-a-time experimentations. For instance, Ngah and Fatinathan (2010), studied the adsorption of Pb (II) using chitosan (and chitosan derivatives beads). They investigated the effects of pH, adsorbent dosage, and initial concentration via one-factor-at-a-time experiments. Although they obtained a similar optimum pH range of 4.5, they could not explain in detail the interactive effects of other factors, such as pH with adsorbent dosage, pH with initial concentration, or adsorbent dosage with initial concentration. Rahimi et al. (2015), studied the optimisation of Pb removal from aqueous solution using goethite/chitosan nanocomposite using Box–Behnken design. Similar to this study, they found that a reduced quadratic model was the best fit for the experimental data, and that pH was the most significant factor affecting the removal efficiency of Pb ions. However, they only investigated the optimisation of these factors with one adsorbent sample and 15 experimental runs were used. If three adsorbent samples were to be used, at least 51 experimental runs would have to be generated for optimisation study of pH, adsorbent dosage, and initial concentration. This would be time-consuming and expensive. In another adsorption study, Aydin and Aksoy (2009) investigated the optimisation of Cr (VI) ions onto chitosan using a Central-Composite design. They investigated the same three adsorption factors, pH, adsorbent dosage, and initial concentration, but with just one adsorbent sample by carrying out 20 batch adsorption experiments. They found that all three factors were significant for the removal efficiency (%) of Cr (VI) ions by chitosan. If three adsorbent samples were to be used, at least 60 experimental runs would have to be generated for optimisation studies of these factors. This again would involve conducting many experiments, which would be time-consuming and

costly. In this study, we simultaneously investigated the optimisation of adsorption parameters (pH, adsorbent dosage, and initial concentration) with three different (but similar) adsorbent samples using just 28 adsorption experiments. This was more efficient and cost-effective.

Since three different adsorbent samples were investigated simultaneously, one may expect that statistical diagnosis (such as ANOVA) containing information about the studied adsorption factors would be obtained for each adsorbent. However, this was not possible, which is a limitation of this study. An advantage of the approach used herein are the Perturbation, 2D contour and 3D surface plots, which help describe and visualise how the significant factors (pH, adsorbent dosage, and initial concentration) affect the adsorption of Pb ions with the respective adsorbents. The trends of these behaviours among the three adsorbents of 90/10 investigated in this study, and those of other samples composed of 70/30 and 50/50 ratios investigated in our previous study (Majiya, 2022), remained similar, but with some slight differences. In addition, although the model equations generated in this study (like all other statistical models) may not perfectly predict actual values when computing factor values due to inherent challenges like noise, model limitations, or complexity, they still offer valuable insights into the influence of each factor.

4.3 Optimisation of adsorption parameters

In this study, the adsorption capacity and adsorption efficiency were simultaneously optimised using a desirability function approach. When the adsorption capacity was chosen as the main priority response, the adsorption efficiency was considered less important. On the other hand, when the adsorption efficiency was considered as a more important response, the adsorption capacity was adjusted as less priority response. Through this, the optimum values of each response together with optimum conditions were achieved for each respective adsorbent. Under optimal conditions, the adsorption capacity of beads-A (73.22 mg/g) and beads-B (77.56 mg/g) was found to be higher than that of their corresponding composites (51.67 mg/g). Although the optimum adsorption capacity values were slightly higher, the trends were similar to those observed for the maximum adsorption capacity (Qmax) values reported in a previous study (Majiya, 2022; Majiya et al., 2023). The slight

differences in the values may be attributed to the deliberate optimisation of experimental conditions usually obtained from the response surface methods (e.g., I-optimal design), compared to the fixed conditions employed during equilibrium experiments. The optimum adsorption efficiency value of about 100% was achievable for all three adsorbents. It's crucial to remember that the estimated optimal response values (i.e. optimum adsorption capacity and efficiency), might not be truly optimal in practice due to potential errors in the estimates and model inadequacies. The simultaneous optimisation of these two responses is key in understanding the absorption behaviour of Pb (II) ions by Bt-Ch composites and beads. Previous literature on the adsorption of heavy metals has mostly used single-response optimisation (Ahmad and Hasan, 2016; Amini et al., 2008; Anupam et al., 2011; Aydin and Aksoy, 2009; Ayushi et al., 2017; Gusain et al., 2014; Rahimi et al., 2015; Yus Azila et al., 2008). However, it is important to consider both adsorption capacity and adsorption efficiency when optimising experimental conditions for the removal of heavy metals. The simultaneous optimisation of these two responses is a more comprehensive approach that can lead to better understanding of the adsorption process. For instance, when removing heavy metals (such as Pb) from drinking water (or wastewater) using Bt-Ch composites/beads, a higher adsorption capacity means that these adsorbents can treat more metal-contaminated water before needing replacement, reducing cost and environmental impact, which remains the primary concern for large-scale water treatment. However, adsorption efficiency might be relevant if you want to ensure the complete removal of heavy metals even with small amounts of adsorbents.

The desirability index values for the optimised conditions were 0.892, 0.964, and 0.974 for the Pb adsorption capacity of Bt-Ch composites, beads-A, and beads-B, respectively, and the desirability index values for the optimised conditions were 0.945, 0.967, and 0.956 for the Pb adsorption efficiency of Bt-Ch composites, beads-A, and beads-B, respectively. All these indexes are very close to unity (1), indicating excellent values that satisfy the optimisation criteria (Beringhs et al., 2015; Myers et al., 2016). Beringhs et al. (2015) found that the optimised conditions for the quantification of phenolic acids in *Cecropia glaziovii* products by IV-optimal design were found under a desirability index of 0.598.

4.4 Adsorption mechanism

The data obtained in this study alone is not sufficient to provide a clear explanation of the adsorption mechanism of Pb onto Bt-Ch composites/beads. However, it did offer optimal experimental conditions for investigating significant factors (including pH and adsorbent dosage) in the author's other related adsorption studies (e.g., equilibrium experiments) in which the adsorption mechanism and a scheme are discussed in more detail (Majiya et al., 2023). Considering the strong effect of pH observed in this study it could infer a stronger Langmuir isotherm influence (Jeppu and Clement, 2012). The Langmuir model characterises adsorption behaviour through two key parameters, the maximum adsorption capacity (Qmax) and the Langmuir constant (KL). Regarding Qmax, as pH increases from 2 to 5, the surface charge of Bt-Ch composites/beads becomes less positive due to the deprotonation of amino functional groups in the chitosan. This reduction in positive charge enhances electrostatic attraction to Pb cations, leading to a higher Qmax value. In terms of KL, these values optimised with at a high level at pH 4.5, indicating strong complexation of the Pb(II) with the amino functional groups. Furthermore, it is appreciated that the adsorption mechanism is complicated especially since there are different adsorption sites associated with either the chitosan or cation exchange site of the montmorillonite within the bentonite. If considering chitosan alone and that at pH 4.5 the amine groups would be protonated (NH_3^+). It would be unlikely for an electrostatic interaction to occur between NH_3^+ and positively charged Pb^{2+} ions in its simplest form. This therefore would support a dominant cation exchange mechanism with the bentonite suggested in our previous study and would be acceptable because the driving force for the cation exchange of Pb^{2+} with Na^+ within the interlayer is the poorer solubility of the $PbNO_3$ in water compared to $NaNO_3$ rather than an electrostatic interaction. Although there is no strong evidence, the complexation with chitosan and Pb(II) could be a possibility. Also, adsorption linked to the slightly polar ether and/or hydroxyl groups of chitosan could not be ruled out at this low pH ≤ 2. Also, when chitosan and bentonite are combined in such close proximity, new complexation adsorption sites could be available.

Overall, this study has shown the use of I-optimal design can be applied as a chemometric tool to simultaneously study the adsorption parameters of Pb (and most likely other metal

ions or with multiple metal ions) with multiple adsorbents. It has provided insight into how the adsorption (adsorbent quality; Pb adsorption capacity) and efficiency of the adsorption process (Pb removal %) can be approached simultaneously in an economic way, and it has also indicated the potential of using Bt-Ch composites/beads as a cost-effective adsorbent for the removal of Pb (II) ions from both drinking and wastewater.

5.0 Conclusion

This study successfully employed I-optimal design to optimise significant adsorption parameters for the removal of Pb ions from aqueous solutions with multiple adsorbents. The study found that the reduced quadratic model equations (generated for each response) adequately describe the behaviour of the adsorption factors (and their interactions) regarding the removal of Pb by Bt-Ch composites/beads. Very small values of CV (%) were observed for both adsorption capacity and adsorption efficiency, suggesting that deviation between the predicted and experimental data values were minimal and highly reproducible. Further statistical analysis revealed that the studied adsorption factors (pH, adsorbent dose, and initial concentration) have a more pronounced effect on the adsorption capacity compared to adsorption efficiency. Adsorbent dosage was found to have the greatest effect on adsorption capacity, while the initial pH of Pb (II) solution had the greatest effect on adsorption efficiency. The results from the confirmation experiments validated the accurate prediction of the quantity of Pb ions removed from aqueous solutions at optimised conditions. The high desirability indexes obtained for adsorption capacity (0.892 – 0.974) and adsorption efficiency (0.945 – 0.967) were highly satisfactory, especially when investigating and optimising multiple responses (and factors) by response surface methodology. The success of the I-optimal design adopted in this study supports the stronger and more cost-effective methods than the typical “one-factor-at-a-time” experimental approach and other response surface methods (e.g., CCD and BBD) previously published in the literature.

A limitation of the study was the inability to perform individual statistical analysis for each adsorbent due to the simultaneous investigation of three different samples. As with all statistical models, care needs to be taken as the generated equations may not perfectly

predict actual values due to inherent challenges such as noise, model limitations, or complexity.

Overall, the study offers valuable insights into the influence of each factor on Pb(II) ion adsorption and provides optimal experimental conditions for subsequent adsorption studies (e.g., adsorption equilibrium). These findings can contribute to a better understanding of the adsorption mechanism and inform the design of more efficient and cost-effective adsorbents for heavy metal removal. In addition, these findings can be useful for the reproduction of the optimised experimental conditions in adsorption science, especially with multiple adsorbents simultaneously. Future studies could explore the competitive adsorption of other metal ions (and other pollutants), and this study described herein could be useful in guiding the design of experiments, especially when dealing with multiple factors, responses, and adsorbents.

Declaration of Competing Interest

The authors declare that they do not have any identified personal or financial conflicts of interest which might have had an impact on the research findings presented in this article.

CRediT authorship contribution statement

Hassan Majiya: Funding acquisition, Conceptualisation, Design of Experiments, Data curation, Writing- Original draft preparation, Writing- Reviewing and Editing

Francis Clegg: Writing- Reviewing and Editing, Supervision.

Chris Sammon: Supervision.

Acknowledgement

Hassan Majiya is grateful to Sheffield Hallam University, UK, for allowing him to conduct his research work for his PhD at the Materials and Engineering Research Institute (MERI). The project is financially supported by Tertiary Education Trust Fund (TETFund) in Nigeria. For the purpose of open access, the author has applied a Creative Commons Attribution (CC BY) licence to any Author Accepted Manuscript version arising from this submission.

Table 1 Factors and their levels investigated during the optimisation stage of the batch adsorption experiments of Pb (II) ions onto Bt-Ch composites/beads

Levels	Numeric continuous factors			Categoric nominal factor
	A-pH	B-Adsorbent dosage (g)	C-Initial concentration (mg/L)	D-Adsorbent type
Low (-1)	2	0.05	50	Bt-Ch composites (X)
Centre point (0)	varied	varied	varied	Bt-Ch beads-A (Y)
High (+1)	5	0.50	250	Bt-Ch beads-B (Z)

Note: The centre points (0) for each continuous factor maybe slightly different due to the algorithms of the Optimal-I designs

Table 2 Confirmation of experimental runs for analysed Optimal-I design model

Response	Target	Predicted Mean	Confirmation experiment	Confidence Interval (95%)	
				Low	High
Pb-Adsorption capacity (mg/g)	Maximise	51.7 ± 2.4	45.6 ± 0.5	45.5	58.6
Pb-Adsorption efficiency (%)	Maximise	50.2 ± 2.8	56.7 ± 2.3	43.1	58.3

Adsorbent type used = Bt-Ch composites (X); pH = 4.5; adsorbent dose = 0.05 g; Initial Pb(II) concentration = 202.9 ~ 205.0 mg/L. For confirmation experiment, each value represents mean ± standard deviation of three (3) different samples (n = 3)

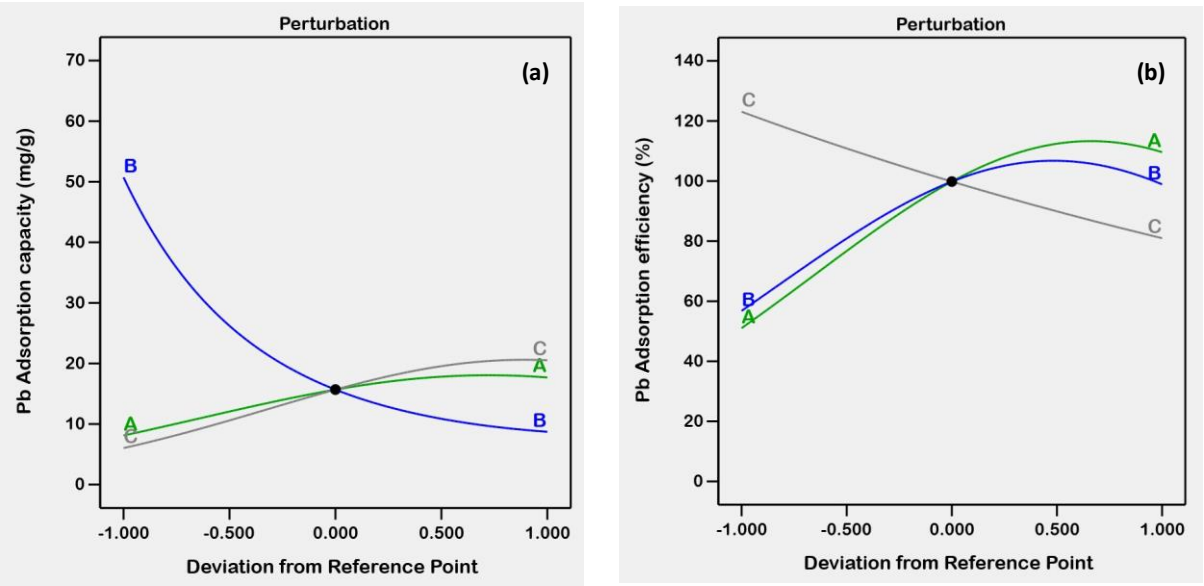

Figure 1 Perturbation plots showing the effect of each factor on the (a) adsorption capacity and (b) adsorption efficiency by Bt-Ch beads-A (adsorbent Y).
Note: these graphs were plotted and obtained from Design-Expert®13; A = pH, B = adsorbent dose, C = initial concentration

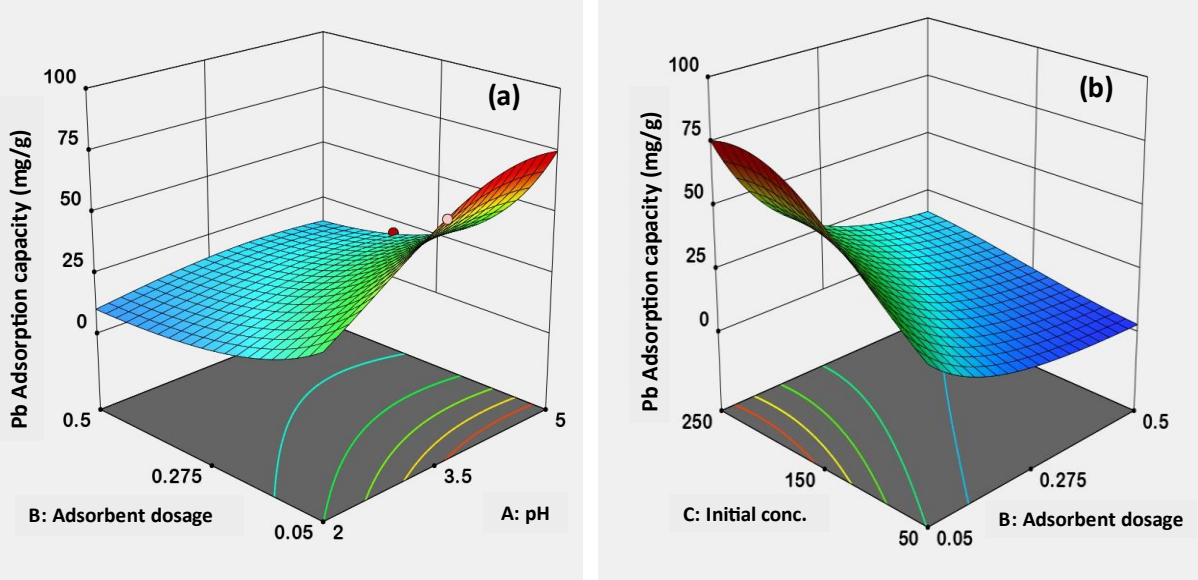

Figure 2 3D response surface plot for the interaction effect on Pb adsorption capacity; (a) pH-adsorbent dosage (at constant 200 mg/L initial conc.) and (b) adsorbent dosage-Initial conc. (at constant pH 4.5) for Bt-Ch beads-B (adsorbent Z). Note: these 3D surface plots were plotted and obtained from the Design-Expert®13 version

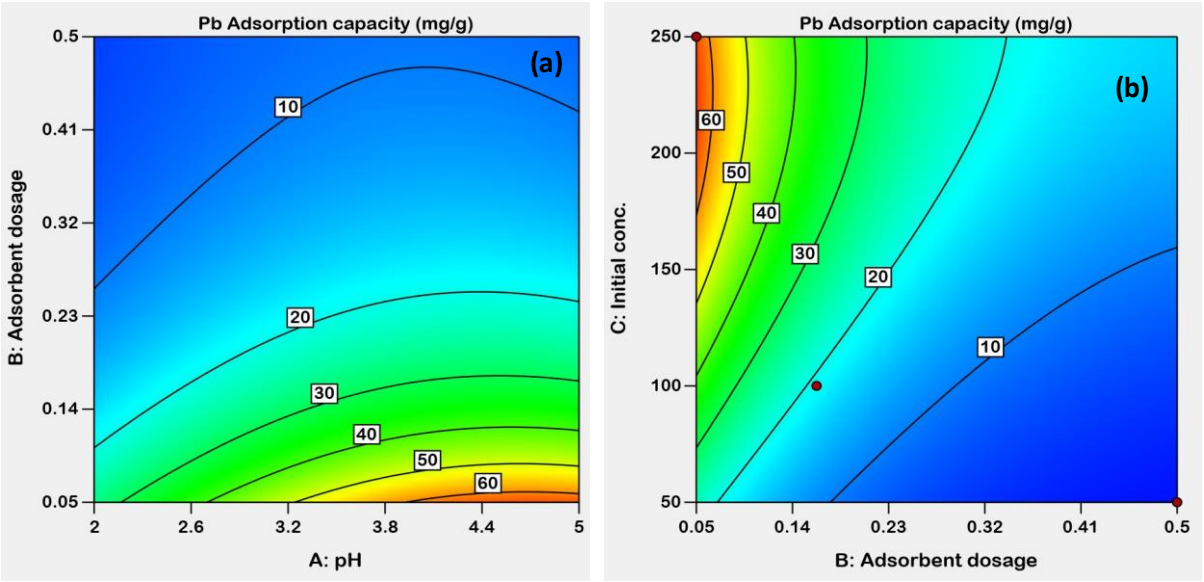

Figure 3 2D contour plots for the interaction effect on Pb adsorption capacity; (a) pH-adsorbent dosage and (b) adsorbent dosage-Initial conc. for Bt-Ch beads-B (adsorbent Z). Note: these 2D contour plots were plotted and obtained from the Design-Expert®13 version

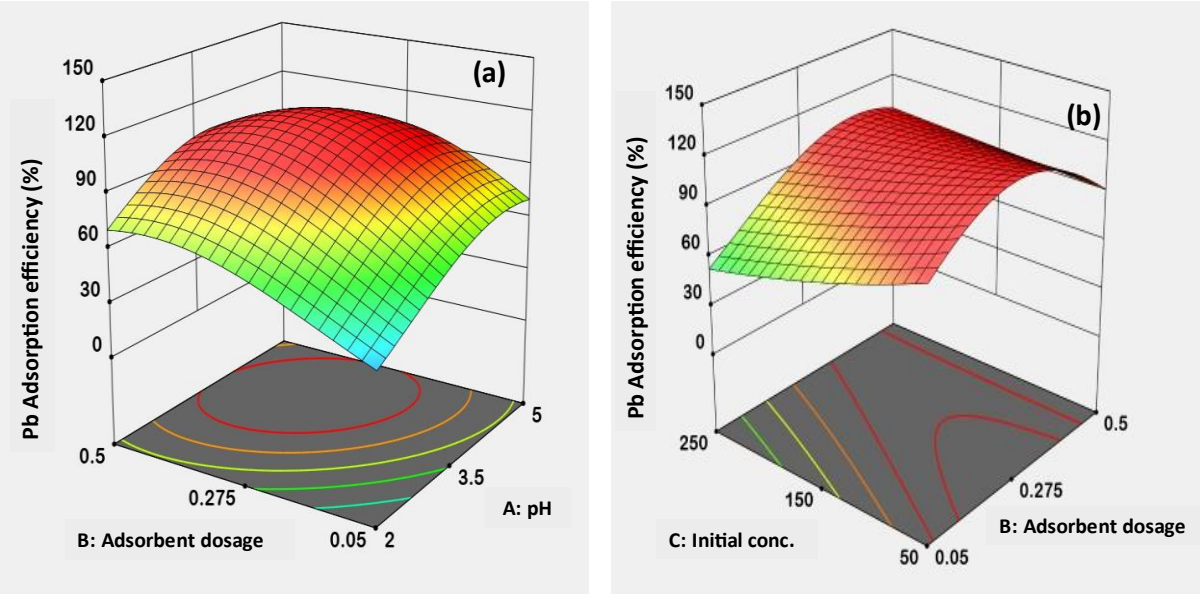

Figure 4 3D response surface plot for the interaction effect on Pb adsorption efficiency (%); (a) pH-adsorbent dosage (at constant 150 mg/L initial conc.) and (b) adsorbent dosage-Initial conc. (at constant pH 4.5) for Bt-Ch beads-B (adsorbent Z). Note: these 3D surface plots were plotted and obtained from the Design-Expert®13 version

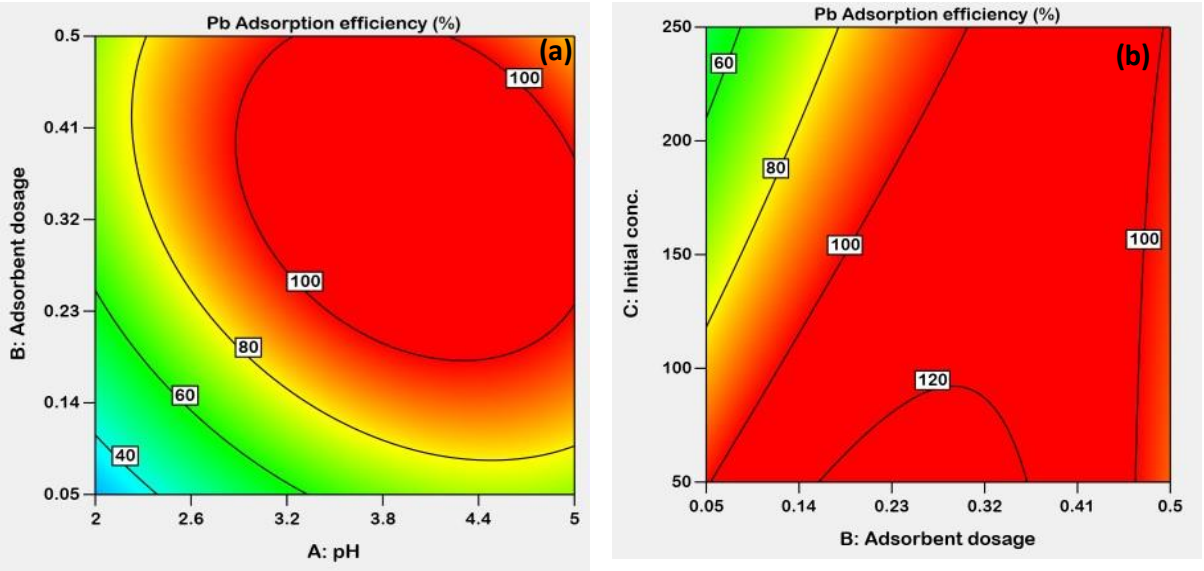

Figure 5 2D contour plots for the interaction effect on Pb adsorption efficiency (%); (a) pH-adsorbent dosage and (b) adsorbent dosage-Initial conc. for Bt-Ch beads-B (adsorbent Z). Note: these 2D contour plots were plotted and obtained from the Design-Expert®13 version

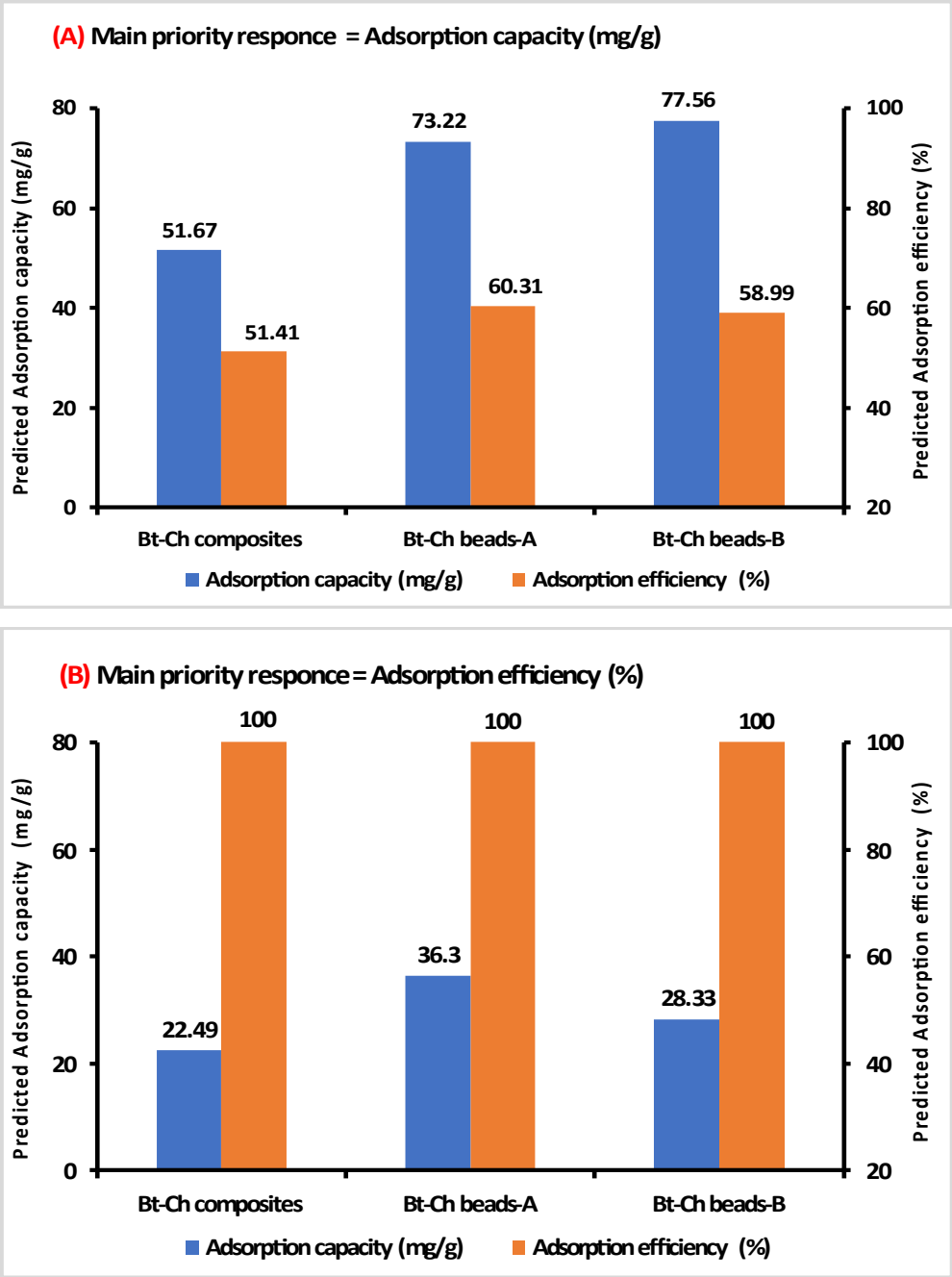

Figure 6 Charts showing (a) adsorption capacity as main priority response (with corresponding adsorption efficiency) and (b) adsorption efficiency as main priority response (with corresponding adsorption capacity) obtained from optimised conditions.

References

Abollino, O., Aceto, M., Malandrino, M., Sarzanini, C., Mentasti, E., 2003. Adsorption of heavy metals on Na-montmorillonite. Effect of pH and organic substances. Water Res. 37, 1619–1627. https://doi.org/10.1016/S0043-1354(02)00524-9

Ahmad, R., Hasan, I., 2016. Optimization of the adsorption of Pb (II) from aqueous solution onto PAB nanocomposite using response surface methodology. Environ. Nanotechnology, Monit. Manag. 6, 116–129. https://doi.org/10.1016/j.enmm.2016.09.002

Ahmadi, A., Heidarzadeh, S., Mokhtari, A.R., Darezereshki, E., Harouni, H.A., 2014. Optimization of heavy metal removal from aqueous solutions by maghemite (γ-Fe2O3) nanoparticles using response surface methodology. J. Geochemical Explor. 147, 151–158. https://doi.org/10.1016/j.gexplo.2014.10.005

Amini, M., Younesi, H., Bahramifar, N., Lorestani, A.A.Z., Ghorbani, F., Daneshi, A., Sharifzadeh, M., 2008. Application of response surface methodology for optimization of lead biosorption in an aqueous solution by Aspergillus niger. J. Hazard. Mater. 154, 694–702. https://doi.org/10.1016/j.jhazmat.2007.10.114

Anfar, Z., El Haouti, R., Lhanafi, S., Benafqir, M., Azougarh, Y., El Alem, N., 2017. Treated digested residue during anaerobic co-digestion of Agri-food organic waste: Methylene blue adsorption, mechanism and CCD-RSM design. J. Environ. Chem. Eng. 5, 5857–5867. https://doi.org/10.1016/j.jece.2017.11.015

Anupam, K., Dutta, S., Bhattacharjee, C., Datta, S., 2011. Adsorptive removal of chromium (VI) from aqueous solution over powdered activated carbon: Optimisation through response surface methodology. Chem. Eng. J. 173, 135–143. https://doi.org/10.1016/j.cej.2011.07.049

Aydin, Y.A., Aksoy, N.D., 2009. Adsorption of chromium on chitosan: Optimization, kinetics and thermodynamics. Chem. Eng. J. 151, 188–194. https://doi.org/10.1016/j.cej.2009.02.010

Ayushi, V., Kumar, S., Kumar, S., 2017. Statistical modeling, equilibrium and kinetic studies of cadmium ions biosorption from aqueous solution using S. filipendula. J. Environ. Chem. Eng. 5, 2290–2304. https://doi.org/10.1016/j.jece.2017.03.044

Bajpai, S., Gupta, S.K., Dey, A., Jha, M.K., Bajpai, V., Joshi, S., Gupta, A., 2012. Application of Central Composite Design approach for removal of chromium (VI) from aqueous solution using weakly anionic resin: Modeling, optimization, and study of interactive variables. J. Hazard. Mater. 227–228, 436–444. https://doi.org/10.1016/j.jhazmat.2012.05.016

Bambaeero, A., Bazargan-Lari, R., 2021. Simultaneous removal of copper and zinc ions by low cost natural snail shell/hydroxyapatite/chitosan composite. Chinese J. Chem. Eng. 33, 221–230. https://doi.org/10.1016/j.cjche.2020.07.066

Ben-Khalifa, E., Rzig, B., Chakroun, R., Nouagui, H., Hamrouni, B., 2019. Application of response surface methodology for chromium removal by adsorption on low-cost biosorbent. Chemom. Intell. Lab. Syst. 189, 18–26. https://doi.org/10.1016/j.chemolab.2019.03.014

Beringhs, A.O., Dalmina, M., Creczynski-Pasa, T.B., Sonaglio, D., 2015. Response surface methodology IV-optimal design applied to the performance improvement of an RP-HPLC-UV method for the quantification of phenolic acids in Cecropia glaziovii products. Rev. Bras. Farmacogn. 25, 513–521. https://doi.org/10.1016/j.bjp.2015.05.007

Chen, L., Wu, P., Chen, M., Lai, X., Ahmed, Z., Zhu, N., Dang, Z., Bi, Y., Liu, T., 2018. Preparation and characterization of the eco-friendly chitosan/vermiculite biocomposite with excellent removal capacity for cadmium and lead. Appl. Clay Sci. 159, 74–82. https://doi.org/10.1016/j.clay.2017.12.050

Design-Expert® software, version 13.0, Stat-Ease, Inc., Minneapolis, MN, USA, www.statease.com.

El Kaim Billah, R., Islam, M.A., Nazal, M.K., Bahsis, L., Soufiane, A., Abdellaoui, Y., Achak, M., 2024. A novel glutaraldehyde cross-linked chitosan@acid-activated bentonite composite for effective Pb (II) and Cr (VI) adsorption: Experimental and theoretical studies. Sep. Purif. Technol. 334, 126094. https://doi.org/10.1016/j.seppur.2023.126094

El KaimBillah, R., Islam, M.A., Agunaou, M., Soufiane, A., 2021. A promising chitosan/fluorapatite composite for efficient removal of lead (II) from an aqueous solution. Arab. J. Geosci. 14. https://doi.org/10.1007/s12517-021-07473-w

Fu, F., Wang, Q., 2011. Removal of heavy metal ions from wastewaters: A review. J. Environ. Manage. 92, 407–418. https://doi.org/10.1016/j.jenvman.2010.11.011

Glyk, A., Solle, D., Scheper, T., Beutel, S., 2015. Optimization of PEG-salt aqueous two-phase systems by design of experiments. Chemom. Intell. Lab. Syst. 149, 12–21. https://doi.org/10.1016/j.chemolab.2015.09.014

Goos Peter, B.J., 2011. Optimal Design of Experiments: A Case Study Approach. John Wiley & Sons, Ltd. https://doi.org/10.2307/2584025

Goupy Jacques, L., 1993. Methods for experimental design: principles and applications for physicist and chemists. Elsevier, Amsterdam, Netherlands.

Gusain, D., Bux, F., Sharma, Y.C., 2014. Abatement of chromium by adsorption on nanocrystalline zirconia using response surface methodology. J. Mol. Liq. 197, 131–141. https://doi.org/10.1016/j.molliq.2014.04.026

Hao, L., Liu, M., Wang, N., Li, G., 2018. A critical review on arsenic removal from water using iron-based adsorbents. RSC Adv. 8, 39545–39560. https://doi.org/10.1039/c8ra08512a

Hassan, M.M., Nuhu, A.A., Sallau, M.S., Majiya, H.M., Mohammed, A.K., 2015. Zamfara lead poisoning saga: Comparison of lead contamination level of water samples and lead poisoning in Bagega Artisanal gold mining district, Nigeria. J. Chem. Pharm. Res. 7, 7–

12.

Jacob, J.M., Karthik, C., Saratale, R.G., Kumar, S.S., Prabakar, D., Kadirvelu, K., Pugazhendhi, A., 2018. Biological approaches to tackle heavy metal pollution: A survey of literature. J. Environ. Manage. 217, 56–70. https://doi.org/10.1016/J.JENVMAN.2018.03.077

Jensen, W.A., 2018. Open problems and issues in optimal design. Qual. Eng. 30, 583–593. https://doi.org/10.1080/08982112.2018.1517884

Jeppu, G.P., Clement, T.P., 2012. A modified Langmuir-Freundlich isotherm model for simulating pH-dependent adsorption effects. J. Contam. Hydrol. 129–130, 46–53. https://doi.org/10.1016/j.jconhyd.2011.12.001

Landdaburu-Aguirre, J., 2012. Micellar-enhanced ultrafiltration for the removal of heavy metals from phosphorous-rich wastewaters : From end-of-pipe to clean technology, Doctoral D. ed. Acta Univ. Oul. C 428, 2012 University of Oulu, P.O. Box 4300, FI-90014 University of Oulu, Finland.

Lata, S., Samadder, S.R., 2016. Removal of arsenic from water using nano adsorbents and challenges: A review. J. Environ. Manage. 166, 387–406. https://doi.org/10.1016/j.jenvman.2015.10.039

Liu, J., Zheng, L., Li, Y., Free, M., Yang, M., 2016. Adsorptive recovery of palladium(II) from aqueous solution onto cross-linked chitosan/montmorillonite membrane. RSC Adv. 6, 51757–51767. https://doi.org/10.1039/c6ra06731j

Liu, Q., Yang, B., Zhang, L., Huang, R., 2015. Adsorption of an anionic azo dye by cross-linked chitosan/bentonite composite. Int. J. Biol. Macromol. 72, 1129–1135. https://doi.org/10.1016/j.ijbiomac.2014.10.008

Liu, W., Ma, B., Li, F., Fu, Y., Tai, J., Zhou, Y., Lei, L., 2016. Reduction of lead dioxide with oxalic acid to prepare lead oxide as the positive electrode material for lead acid batteries. RSC Adv. 6, 108513–108522. https://doi.org/10.1039/c6ra23671e

Lourdes Dalida, M.P., Francia Mariano, A. V, Futalan, C.M., Kan, C.-C., Tsai, W.-C., Wan, M.-W., 2011. Adsorptive removal of Cu(II) from aqueous solutions using non-crosslinked and crosslinked chitosan-coated bentonite beads. DES 275, 154–159. https://doi.org/10.1016/j.desal.2011.02.051

Majdoubi, H., EL Kaim Billah, R., Aminul Islam, M., Nazal, M.K., Shekhawat, A., Alrashdi, A.A., Alberto Lopez-Maldonado, E., Soulaimani, A., Tamraoui, Y., Jugade, R., Lgaz, H., 2023. An eco-friendly chitosan-diethylaminoethyl cellulose composite: In-depth analysis of lead (II) and arsenic(V) decontamination from water with molecular perspectives. J. Mol. Liq. 387, 122680. https://doi.org/10.1016/j.molliq.2023.122680

Majiya, H., 2022. Remediation of Heavy Metals from Water using Modified Clay-Chitosan Composites. PhD Thesis, Sheffield Hallam University, United Kingdom. https://doi.org/10.7190/shu-thesis-00533

Majiya, H., Chowdhury, K.F., Stonehouse, N.J., Millner, P., 2019. TMPyP functionalised chitosan membrane for efficient sunlight driven water disinfection. J. Water Process

Eng. 30, 100475. https://doi.org/10.1016/j.jwpe.2017.08.013

Majiya, H., Clegg, F., Sammon, C., 2023. Bentonite-Chitosan composites or beads for lead (Pb) adsorption : Design , preparation , and characterisation. Appl. Clay Sci. 246, 107180. https://doi.org/10.1016/j.clay.2023.107180

Majiya, H.M., 2017. Photosensitiser functionalised nanofiber fabric for efficient light driven water disinfection. PhD Thesis, University of Leeds, United Kingdom. https://doi.org/uk.bl.ethos.749407

Maleki, S., Karimi-Jashni, A., 2020. Optimization of Ni(II) adsorption onto Cloisite Na+ clay using response surface methodology. Chemosphere 246, 125710. https://doi.org/10.1016/j.chemosphere.2019.125710

Mancenido, M. V., Pan, R., Montgomery, D.C., Anderson-Cook, C.M., 2019. Comparing D-optimal designs with common mixture experimental designs for logistic regression. Chemom. Intell. Lab. Syst. 187, 11–18. https://doi.org/10.1016/j.chemolab.2019.02.003

Montgomery, D.C., 2013. Design and Analysis of Experiments, ninth ed. John Wiley & Sons, Inc.

Morgan, E., 1991. Chemometrics: experimental design (analytical chemistry by open learning). Wiley–Blackwell, Chichester.

Morgan, E., Burton, K.W., Church, P.A., 1989. Practical exploratory experimental designs. Chemom. Intell. Lab. Syst. 5, 283–302. https://doi.org/10.1016/0169-7439(89)80028-0

Myers, R.H., Montgomery, D.C., Anderson-Cook, C.M., 2016. Response Surface Methodology: Process and Product Optimization Using Designed Experiments, 4th ed. Wiley & Sons Inc.

Ngah, W.S.W., Fatinathan, S., 2010. Pb(II) biosorption using chitosan and chitosan derivatives beads: Equilibrium, ion exchange and mechanism studies. J. Environ. Sci. 338–346. https://doi.org/10.1016/S1001-0742(09)60113-3

Ngah, W.S.W., Fatinathan, S., 2009. Adsorption characterization of Pb(II) and Cu(II) ions onto chitosan-tripolyphosphate beads: Kinetic, equilibrium and thermodynamic studies. J. Environ. Manage. 91, 658–969. https://doi.org/10.1016/j.jenvman.2009.12.003

Nonkumwong, J., Ananta, S., Srisombat, L., 2016. Effective removal of lead(II) from wastewater by amine-functionalized magnesium ferrite nanoparticles. RSC Adv. 6, 47382–47393. https://doi.org/10.1039/c6ra07680g

Nuhu, A.A., Sallau, M.S., Majiya, M.H., 2014. Heavy metal pollution: The environmental impact of artisanal gold mining on Bagega Village of Zamfara State, Nigeria. Res. J. Pharm. Biol. Chem. Sci. 5, 306–313.

Pillai, C.K.S., Paul, W., Sharma, C.P., 2009. Chitin and chitosan polymers: Chemistry, solubility and fiber formation. Prog. Polym. Sci. 34, 641–678. https://doi.org/10.1016/j.progpolymsci.2009.04.001

Pooladi, A., Bazargan-Lari, R., 2023. Adsorption of zinc and copper ions simultaneously on a low-cost natural chitosan/hydroxyapatite/snail shell/nano-magnetite composite. Cellulose 30, 5687–5705. https://doi.org/10.1007/s10570-023-05219-3

Pooladi, A., Bazargan-Lari, R., 2020. Simultaneous removal of copper and zinc ions by Chitosan/Hydroxyapatite/nano-Magnetite composite. J. Mater. Res. Technol. 9, 14841–14852. https://doi.org/10.1016/j.jmrt.2020.10.057

Popuri, S.R., Vijaya, Y., Boddu, V.M., Abburi, K., 2008. Adsorptive removal of copper and nickel ions from water using chitosan coated PVC beads. https://doi.org/10.1016/j.biortech.2008.05.041

Radnia, H., Ghoreyshi, A.A., Younesi, H., Najafpour, G.D., 2012. Adsorption of Fe(II) ions from aqueous phase by chitosan adsorbent: Equilibrium, kinetic, and thermodynamic studies. Desalin. Water Treat. 50, 348–359. https://doi.org/10.1080/19443994.2012.720112

Rahimi, S., Moattari, R.M., Rajabi, L., Derakhshan, A.A., 2015. Optimization of lead removal from aqueous solution using goethite/chitosan nanocomposite by response surface methodology. Colloids Surfaces A Physicochem. Eng. Asp. 484, 216–225. https://doi.org/10.1016/j.colsurfa.2015.07.063

Rusmin, R., Sarkar, B., Liu, Y., Mcclure, S., Naidu, R., 2015. Structural evolution of chitosan-palygorskite composites and removal of aqueous lead by composite beads. Appl. Surf. Sci. 353, 363–375. https://doi.org/10.1016/j.apsusc.2015.06.124

Sallau, M., Majiya, M., Nuhu, A., 2014. Mercury, Cadmium and Nickel Contamination Levels in Water Samples of Bagega Artisanal Gold Mining Communities: The Environmental Health Importance. Res. J. Pharm. Biol. Chem. Sci. 5, 531–536.

Sarkar, M., Majumdar, P., 2011. Application of response surface methodology for optimization of heavy metal biosorption using surfactant modified chitosan bead. Chem. Eng. J. 175, 376–387. https://doi.org/10.1016/j.cej.2011.09.125

Sharma, A.K., Lee, B.K., 2013. Lead sorption onto acrylamide modified titanium nanocomposite from aqueous media. J. Environ. Manage. 128, 787–797. https://doi.org/10.1016/j.jenvman.2013.06.030

Smucker, B., Krzywinski, M., Altman, N., 2018. Optimal experimental design. Nat. Methods 15, 559–560. https://doi.org/10.1038/s41592-018-0083-2

Surchi, K.M.S., 2011. Agricultural Wastes as Low Cost Adsorbents for Pb Removal: Kinetics, Equilibrium and Thermodynamics. Int. J. Chem. 3, 103–112. https://doi.org/10.5539/ijc.v3n3p103

Wang, J., Wang, L., Yu, H., -Ul-Abdin, Z., Chen, Y., Chen, Q., Zhou, W., Zhang, H., Chen, X., 2016. Recent progress on synthesis, property and application of modified chitosan: An overview. Int. J. Biol. Macromol. 88, 333–344. https://doi.org/10.1016/j.ijbiomac.2016.04.002

Wang, S., Dong, Y., He, M., Chen, L., Yu, X., 2008. Characterization of GMZ bentonite and its

application in the adsorption of Pb(II) from aqueous solutions. Appl. Clay Sci. 43, 164–171. https://doi.org/10.1016/j.clay.2008.07.028

Yang, H., Lu, M., Chen, D., Chen, R., Li, L., Han, W., 2020. Efficient and rapid removal of Pb2+ from water by magnetic Fe3O4@MnO2 core-shell nanoflower attached to carbon microtube: Adsorption behavior and process study. J. Colloid Interface Sci. 563, 218–228. https://doi.org/10.1016/j.jcis.2019.12.065

Yang, S., Zhao, D., Zhang, H., Lu, S., Chen, L., Yu, X., 2010. Impact of environmental conditions on the sorption behavior of Pb(II) in Na-bentonite suspensions. J. Hazard. Mater. 183, 632–640. https://doi.org/10.1016/j.jhazmat.2010.07.072

Yus Azila, Y., Mashitah, M.D., Bhatia, S., 2008. Process optimization studies of lead (Pb(II)) biosorption onto immobilized cells of Pycnoporus sanguineus using response surface methodology. Bioresour. Technol. 99, 8549–8552. https://doi.org/10.1016/j.biortech.2008.03.056

Zbair, M., Anfar, Z., Ahsaine, H.A., 2019. Reusable bentonite clay: modelling and optimization of hazardous lead and p-nitrophenol adsorption using a response surface methodology approach. RSC Adv. 9, 5756–5769. https://doi.org/10.1039/c9ra00079h

Graphical Abstract